Photopion production with nonresonant Δ_{33} background interference

Joseph L. Sabutis
Department of Physics and Astronomy, University of Pittsburgh, Pittsburgh, Pennsylvania 15260
(Received 28 June 1982)

The nonresonant interference effects in the (3,3) channel proposed by Olsson are incorporated into a full amplitude that describes photopion production from a single nucleon. The reactions $p(\gamma,\pi^+)n$, $n(\gamma,\pi^-)p$, and $p(\gamma,\pi^0)p$ are all well described by this amplitude. The charged pion production cross sections obtained with Olsson's effects are similar to those calculated by Blomqvist and Laget, but the new amplitude has the added feature of also describing neutral pion production. Asymmetry parameters calculated with the new and Blomqvist and Laget amplitudes are compared with experiment for the cases where either the incident photon, the target, or final state baryon are polarized; the new photopion production amplitude provides a good description of these experiments.

[NUCLEAR REACTIONS Photopion production amplitude, (γ,π) cross sections, polarization calculations.]

I. INTRODUCTION

The Blomqvist-Laget (BL) operator[1] successfully describes charged (γ,π) production from a target nucleon and is the starting point for many nuclear calculations. The first such application[2] resulted in good agreement between theory and experiment for the production of charged pions from light nuclei.[3] Sensitivity to the basic photopion dynamics has been revealed by interesting interference effects in the radiative capture of inflight pions on ^{15}N and ^{13}C.[4] However, recent cases have indicated that a more precise description of the photopion production on a nucleon is now needed.[5] An example of its limitation is that the BL description of neutral pion photoproduction from a target proton yields only qualitative agreement with data when calculated with the same parameters as charged pion photoproduction.[6] The inability of the BL amplitude to describe (γ,π^0) production from a proton is one of the major motivations for the construction of the new amplitude in this paper. In charged (γ,π) production, the leading terms obtained from the (Born) diagrams in Fig. 1(a) provide an adequate description of the photopion production process at center of mass (c.m.) energies below the Δ_{33}. However, above the Δ_{33}, terms are not present when one calculates (γ,π^0) from a proton. Here the contribution of the diagrams in Fig. 1(a) is comparable to the contribution of the Δ_{33} arising from Fig. 1(b). The viewpoint taken here is that a modification of the Δ_{33} in the photopion production amplitude is needed to equally treat charged and neutral (γ,π) production. To ascertain the role of the Δ_{33} in the (γ,π) process, one notes that Olsson[7] has shown there is interference between the resonance and the background in the $J=\frac{3}{2}$, $I=\frac{3}{2}$ (3,3) channel in both pion nucleon elastic scattering and photopion production, and gives a parametrization of the dominant multipoles in that particular channel. The amplitude constructed here incorporates Olsson's interference effect into a full photopion production amplitude. This inclusion of Olsson's effect proves to unify the description of charged and neutral (γ,π) production from a single nucleon, give better agreement with neutral pion photoproduction, and yield better agreement with

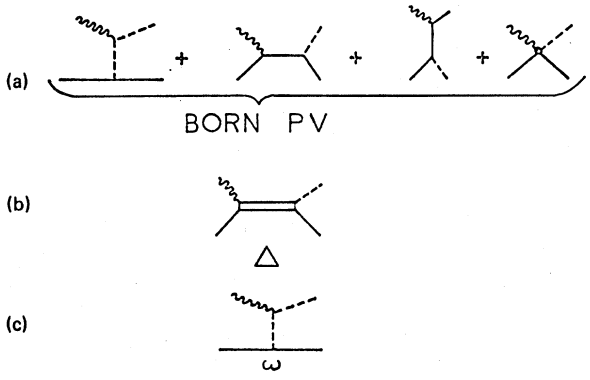

FIG. 1. (a) The Born diagrams, (b) the Δ_{33} diagram, and (c) the ω diagram.

photopion polarization data. The merits of the full photopion production amplitude will hopefully be realized in situations that are particularly sensitive to higher order corrections in the photopion operator strengths, such as neutral pion production from a single nucleon or the case of ^{14}N where the leading terms of the photopion amplitude are suppressed.

As will be explained in Sec. II, the BL photopion production amplitude is calculated in the appropriate nonrelativistic limit of the set of diagrams that appear in Fig. 1. The advantage of using diagrams to obtain the photopion production amplitude, in contrast to a dispersion calculation, is that diagrams provide both a physical picture of the photopion process and guidance as to the frame dependence, which is needed for nuclear applications. However, the unfortunate feature of using lowest order diagrams is that the Δ_{33} resonance [Fig. 1(b)] does not come out of the theory naturally, as it would in the dispersion method,[8-10] but it is put in "by hand." For this reason, care must be taken when adding the contribution from each of the diagrams in Fig. 1 with the correct phases. A consequence of the Watson theorem[10] is that the contribution of the Δ_{33} resonance to the BL photopion production amplitude is constrained by the pion nucleon elastic phase shifts; in this way the imaginary part of the BL photopion amplitude is generated. The photopion amplitude presented in this paper departs from the BL treatment in that the resonant contribution is not supplied by the Δ_{33} diagram in Fig. 1(b); instead the multipoles calculated by Olsson are used to describe the (3,3) channel. Assuming that the background in (γ,π) is given entirely by the Born terms [Fig. 1(a)] projected into the isospin $(I)=\frac{3}{2}$ channel, the experimental values of the pion nucleon elastic phase shifts in the (3,3) channel, δ_{33}, constrain not only the Δ_{33} contribution to the photopion production amplitude, but also the contribution of the nonresonant background. With this change, a new amplitude is constructed which unifies both charged and neutral pion photoproduction by treating the processes with one set of parameters. In contrast, BL required two different sets of parameters, one for charged and another for neutral photopion production, to achieve a satisfactory fit to data.

In polarized (γ,π) experiments, the polarization observables depend on the imaginary part of the photopion production amplitude. Since the BL and new amplitudes differ in both their real and imaginary parts, a sensitive way of checking an amplitude's ability to describe photopion production is by comparing calculations to polarization experiments. Three types of polarization data are examined: polarized photon, polarized target, and final state baryon polarization experiments.

Section II presents the construction of the full photopion production operator along with a discussion of the differences between it and the original BL operator. In Sec. III the results obtained with the new operator are compared to photopion production cross sections and polarization data. Conclusions about the photopion production process deduced from the new operator are presented in Sec. IV.

II. THE FULL PHOTOPION PRODUCTION AMPLITUDE

The BL amplitude is obtained by calculating the nonrelativistic limit of the set of diagrams shown in Fig. 1. In the nonrelativistic limit, terms of order p/m, p being either the initial or final state nucleon three-momentum and m being the nucleon mass, are retained in the vertex operator, nucleon wave function, and numerator of the propagators. In the denominator of the nucleon propagators, terms of order p^2/m^2 are kept for the forward time case and of order p/m for the backward time case. Figure 1(a) shows the four Born terms to be calculated with pseudovector (PV) coupling in the πNN vertex. Figure 1(b) shows the Δ_{33} contribution, which is generated independently of the Born terms. Figure 1(c) shows the ω meson's contribution to the amplitude, which is needed for neutron photopion production. The ω is neutral, but since it is a vector particle, it couples to the photon through its magnetic moment. Invoking the Watson theorem[11] (which states that for a center of mass energy w, below the two pion production threshold, a photopion production amplitude of given parity, isospin, and total angular momentum must have the same phase as the pion-nucleon elastic scattering amplitude with the same quantum numbers), the pion nucleon phase shifts are used by BL to constrain the real and imaginary parts of the Δ_{33} contribution to the photopion production amplitude.

The construction of the new photopion production operator is carried out in the following manner: The procedure is to replace the BL (3,3) channel, Δ_{33}, and background by Olsson's parametrization. To do this, it is assumed that in the BL procedure described above, all multipoles are reproduced except the two dominant ones in the (3,3) channel, the magnetic $L^J=1^{1+1/2}$ and electric $L^J=1^{1+1/2}$. Instead of the BL result, the M_{1+} and the E_{1+} multipoles are taken to be those calculated by Olsson.[7] Since the nonresonance background in Olsson's M_{1+} and E_{1+} is given by the Born term projected into this (3,3) channel, one avoids double counting in this construction by subtracting the M_{1+}^{Born} $(I=\frac{3}{2})$

and E_{1+}^{Born} $(I=\frac{3}{2})$ multipoles from the amplitude calculated from the diagrams in Fig. 1(a). The extraction of the M_{1+}^{Born} $(I=\frac{3}{2})$ and E_{1+}^{Born} $(I=\frac{3}{2})$ multipoles is outlined in the Appendix.

The photopion production amplitude in the c.m. frame, F, is a spin space operator, and using the notation of Chew, Goldberger, Low, and Nambu,[10] is given below in terms of the strengths $F_1 \cdots F_4$:

$$F=\{i(\vec{\sigma}\cdot\vec{\epsilon})F_1+(\vec{\sigma}\cdot\hat{q})[\vec{\sigma}\cdot(\hat{k}\times\vec{\epsilon})]F_2+i(\vec{\sigma}\cdot\hat{k})(\hat{q}\cdot\vec{\epsilon})F_3+i(\vec{\sigma}\cdot\hat{q})(\hat{q}\cdot\vec{\epsilon})F_4\} \ . \tag{1}$$

$\hat{q}$ and $\hat{k}$ are unit vectors in the direction of the c.m. momenta of the pion and photon, respectively, $\vec{\sigma}$ is the Pauli spin operator, and $\vec{\epsilon}$ is the photon polarization vector. The F_i's are then decomposed in isospin:

$$F_i(\gamma p\to n\pi^+)=\sqrt{2}[F_i(I=0)+\tfrac{1}{3}F_i(I=\tfrac{1}{2})-\tfrac{1}{3}F_i(I=\tfrac{3}{2})] \ , \tag{2a}$$

$$F_i(\gamma p\to p\pi^0)=F_i(I=0)+\tfrac{1}{3}F_i(I=\tfrac{1}{2})+\tfrac{2}{3}F_i(I=\tfrac{3}{2}) \ , \tag{2b}$$

$$F_i(\gamma n\to p\pi^-)=\sqrt{2}[F_i(I=0)-\tfrac{1}{3}F_i(I=\tfrac{1}{2})+\tfrac{1}{3}F_i(I=\tfrac{3}{2})] \ , \tag{2c}$$

$$F_i(\gamma n\to n\pi^0)=F_i(I=0)+\tfrac{1}{3}F_i(I=\tfrac{1}{2})+\tfrac{2}{3}F_i(I=\tfrac{3}{2}) \ . \tag{2d}$$

Denoting the strengths calculated from the Born diagrams in Fig. 1(a) plus the ω diagram in Fig. 1(c) by $F_i^{\text{Born}+\omega}$, the new strengths are obtained by subtracting out the nonresonance (3,3) terms obtained in Fig. 1(a), and adding Olsson's description of the M_{1+} and E_{1+} multipoles

$$F_1^{\text{new}}=F_1^{\text{Born}+\omega}+3\cos\theta C_\pi C_\gamma[M_{1+}+E_{1+}-M_{1+}^{\text{Born}}(I=\tfrac{3}{2})-E_{1+}^{\text{Born}}\ (I=\tfrac{3}{2})] \ , \tag{3a}$$

$$F_2^{\text{new}}=F_2^{\text{Born}+\omega}+2C_\pi C_\gamma[M_{1+}-M_{1+}^{\text{Born}}\ (I=\tfrac{3}{2})] \ , \tag{3b}$$

$$F_3^{\text{new}}=F_3^{\text{Born}+\omega}+3C_\pi C_\gamma[E_{1+}-M_{1+}+M_{1+}^{\text{Born}}\ (I=\tfrac{3}{2})-E_{1+}^{\text{Born}}\ (I=\tfrac{3}{2})] \ , \tag{3c}$$

$$F_4^{\text{new}}=F_4^{\text{Born}+\omega} \ . \tag{3d}$$

θ is the angle between $\vec{q}$ and the c.m. momentum of the phonon $\vec{k}$; M_{1+}^{Born} $(I=\frac{3}{2})$ and E_{1+}^{Born} $(I=\frac{3}{2})$ are projections into the (3,3) channel and are given in the Appendix. The M_{1+} and the E_{1+} are the multipoles given by Olsson and they include the Δ_{33} and the nonresonant background contributions to the amplitude

$$M_{1+}=N_M q^{-1}e^{i\delta_{33}}\sin[\delta_{33}+\delta_p^M-\delta_e] \ , \tag{4a}$$

$$E_{1+}=N_E q^{-1}e^{i\delta_{33}}\sin[\delta_{33}+\delta_p^E-\delta_e] \ . \tag{4b}$$

$N_{M,E}$ is the ratio of formation and decay vertices for the specific multipole and the magnetic of the pion momentum, q, is in inverse Fermi. The $C_\pi C_\gamma$ are the isospin coefficients for the $I=\frac{3}{2}$ channel and are given by

$$C_\pi C_\gamma=\begin{cases} \frac{2}{3}\gamma p\to p\pi^0 \ , \\ \frac{2}{3}\gamma n\to n\pi^0 \ , \\ -\sqrt{2}/3\gamma p\to n\pi^+ \ , \\ \sqrt{2}/3\gamma n\to p\pi^- \ . \end{cases} \tag{5}$$

The photopion production background phase $\delta_p^{M,E}$ and the elastic background phase δ_e are derived in Ref. 6 in terms of models that can account for all of the nonresonant photopion production multipoles[12] and pion nucleon elastic low-energy parameters[13,14] such as subthreshold expansion coefficients, scattering lengths, and low-energy phase shifts.

Figure 2 shows the δ_{33} parametrization of the pion-nucleon elastic phase shifts used in reproducing Olsson's M_{1+} and E_{1+}. The multipoles described in Eqs. (4a) and (4b) and the data are shown in Figs. 3(a) and (b). Table I provides a list of parameters used in the BL and the new photopion production operators. M_Δ is the mass of the Δ_{33} resonance, Γ_0 is the width of the Δ_{33} at resonant energy, g_i is the

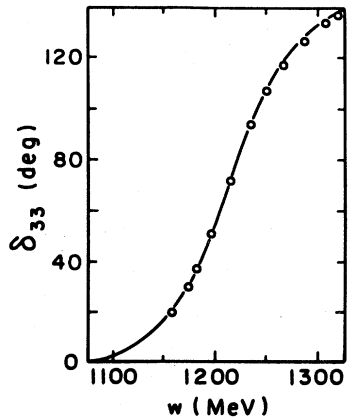

FIG. 2. The parametrization of the 33 phase shifts used in reproducing Olsson's multipoles. Data are from Ref. 16.

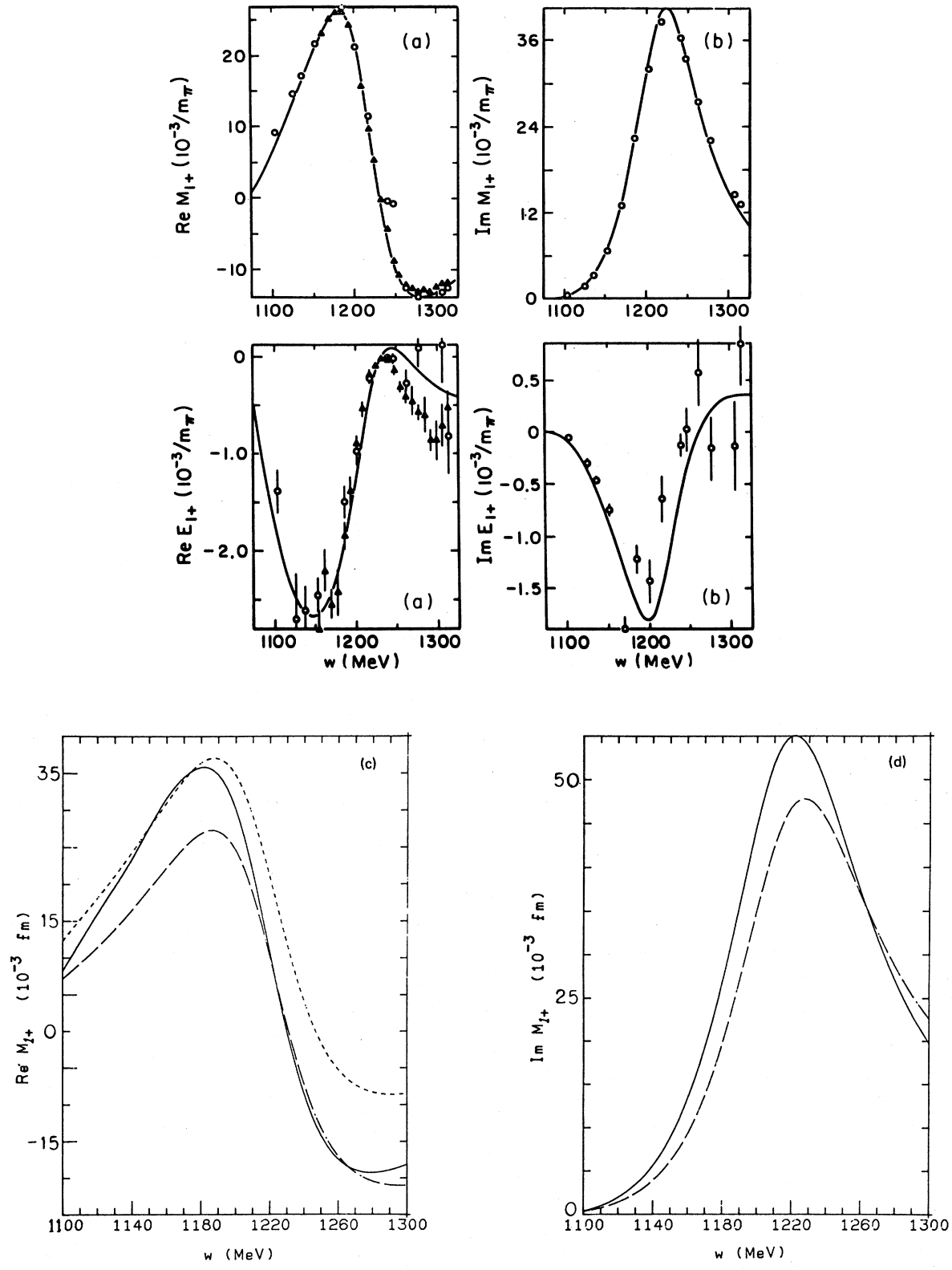

FIG. 3. The (a) real and (b) imaginary parts of M_{1+} ($I=\frac{3}{2}$) and E_{1+} ($I=\frac{3}{2}$); data are from Refs. 17 and 18. Comparison of the new and BL M_{1+} ($I=\frac{3}{2}$) multipole (c) real part and (d) imaginary part.

TABLE I. α is equal to $\frac{1}{137}$ and Ψ_1 is equal to $0.01q(1.07+0.0138q)$ and is in degrees, when q is expressed in MeV/c.

	$\pi^{\pm}$		π^0		
	New	BL	New	BL(A)	BL(B)
M_Δ	1231 MeV	1231 MeV	1231 MeV	1231 MeV	1225 MeV
Γ_0	109 MeV	110 MeV	109 MeV	109 MeV	110 MeV
g_3	2.13	2.13	2.13	2.13	2.18
g_1	0.282	0.282	0.282	0.282	$0.340e^{i\Psi}1$
$g_{\omega 1}$			7.0	17.5	10.0
$g_{\omega 3}$			$0.374\sqrt{4\pi\alpha}$	$0.374\sqrt{4\pi\alpha}$	$0.374\sqrt{4\pi\alpha}$
R	5.30 GeV^{-1}	5.52 GeV^{-1}	5.30 GeV^{-1}	5.52 GeV^{-1}	7.00 GeV^{-1}

$\pi\Delta N$ vertex strength, g_3 is the $\gamma\Delta N$ vertex strength, $g_{\omega 1}$ is the ωNN vertex strength, and $g_{\omega 3}$ is the $\gamma\omega\pi^0$ vertex strength. The parameter R is used in reproducing the δ_{33} phase shifts. To produce a better fit to the neutral pion production data, BL modified their amplitude using a different set of parameters than for charged pion production; those neutral pion production parameters are labeled in Table I by BL(B). The parameters used in the new amplitude were chosen to aggree with BL charged pion production; this was done to emphasize the fact that the same parameters fit to charged pion production could be used as well to predict neutral pion production. With these charged pion production parameters, the product $g_{\omega 1}g_{\omega 3}$ was adjusted in the new amplitude to obtain a good fit to neutral pion production data at 90 deg [Fig. 5(a)].

The imaginary part of the photopion production amplitude plays an important role in the description of the polarization quantities (these are defined in Sec. III); the imaginary part arises from the M_{1+} and E_{1+} multipoles in the $I=\frac{3}{2}$ channel. Figures 3(c) and (d) show as comparison of the M_{1+} multiple used in the new and BL amplitudes. In both these figures, the solid line denotes the M_{1+}^{new} multiple and the dashed line denotes the M_{1+}^{BL} multipole. In Fig. 3(c) the short dashed line denotes the sum of $M_{1+}^{\text{BL}}+M_{1+}^{\text{Born}}$ $(I=\frac{3}{2})$ multipoles, where M_{1+}^{Born} $(I=\frac{3}{2})$ is the contribution to the M_{1+} multipole from the Born diagrams, Fig. 1(a), and the Appendix. The BL amplitude contains no Δ_{33} contribution to the E_{1+} multipole in the $I=\frac{3}{2}$ channel.

III. RESULTS

Comparison of the BL and new photopion production amplitudes is done by looking at the three reactions $p(\gamma,\pi^0)p$, $p(\gamma,\pi^+)n$, and $n(\gamma,\pi^-)p$. Figures 4(a)–(c) give the total cross section as a function of the invariant c.m. energy w, and Figs. 5–7 give the differential cross section as a function of c.m. angle, for different values of w, for these three processes. The solid lines in Figs. 4–10 denote the results obtained with the new photopion production amplitude; the dashed lines denote results obtained with the BL amplitude using parameters labeled by BL(A) in Table I. The dotted lines in Fig. 5(a)–(e) show the calculation for neutral pion production with the parameters listed under BL(B) in Table I. It is seen from these figures that the photopion production amplitude described here does just as well as the BL amplitude for charged pion production and better describes neutral pion production from a proton.

Figures 8–10 give the results from the two amplitudes compared to data from three types of polarization experiments. The data in Fig. 8 are from photon polarization experiments, where the asymmetry parameter is defined as

$$\Sigma(\theta)=\frac{\sigma_\perp(\theta)-\sigma_{||}(\theta)}{\sigma_\perp(\theta)+\sigma_{||}(\theta)}\ . \tag{6}$$

$\sigma_\perp$ ($\sigma_{||}$) is the differential cross section for producing a pion in a plane perpendicular (parallel) to the polarization plane of the incident photon. Except in Fig. 8(a), the new photopion production operator follows the data while BL is low at large c.m. energies. Figure 8(a) will be discussed in the next section.

The data in Fig. 9 are from target polarization experiments, where the asymmetry parameter is defined here as

$$T(\theta)=\frac{\sigma_\uparrow(\theta)-\sigma_\downarrow(\theta)}{\sigma_\uparrow(\theta)+\sigma_\downarrow(\theta)}\ . \tag{7}$$

$\sigma_\uparrow$ ($\sigma_\downarrow$) is the differential cross section for the target polarized parallel (antiparallel) to the direction of $\vec{k}\times\vec{q}$, where $\vec{k}$ and $\vec{q}$ are the c.m. momenta of the photon and pion, respectively. Here again the new

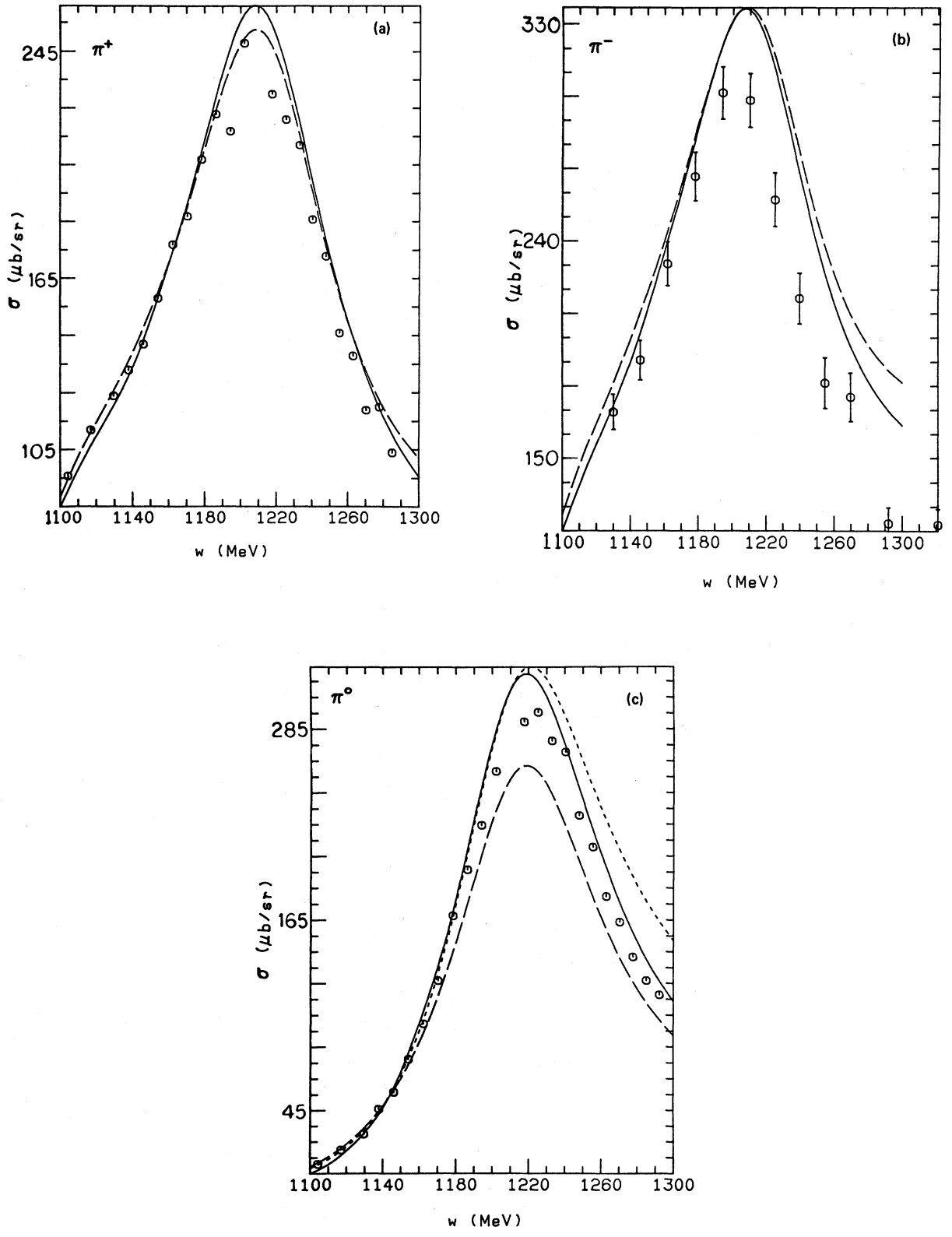

FIG. 4. Total cross section for the photoproduction of (a) π^+, (b) π^-, and (c) π^0. Data are from Refs. 19–24.

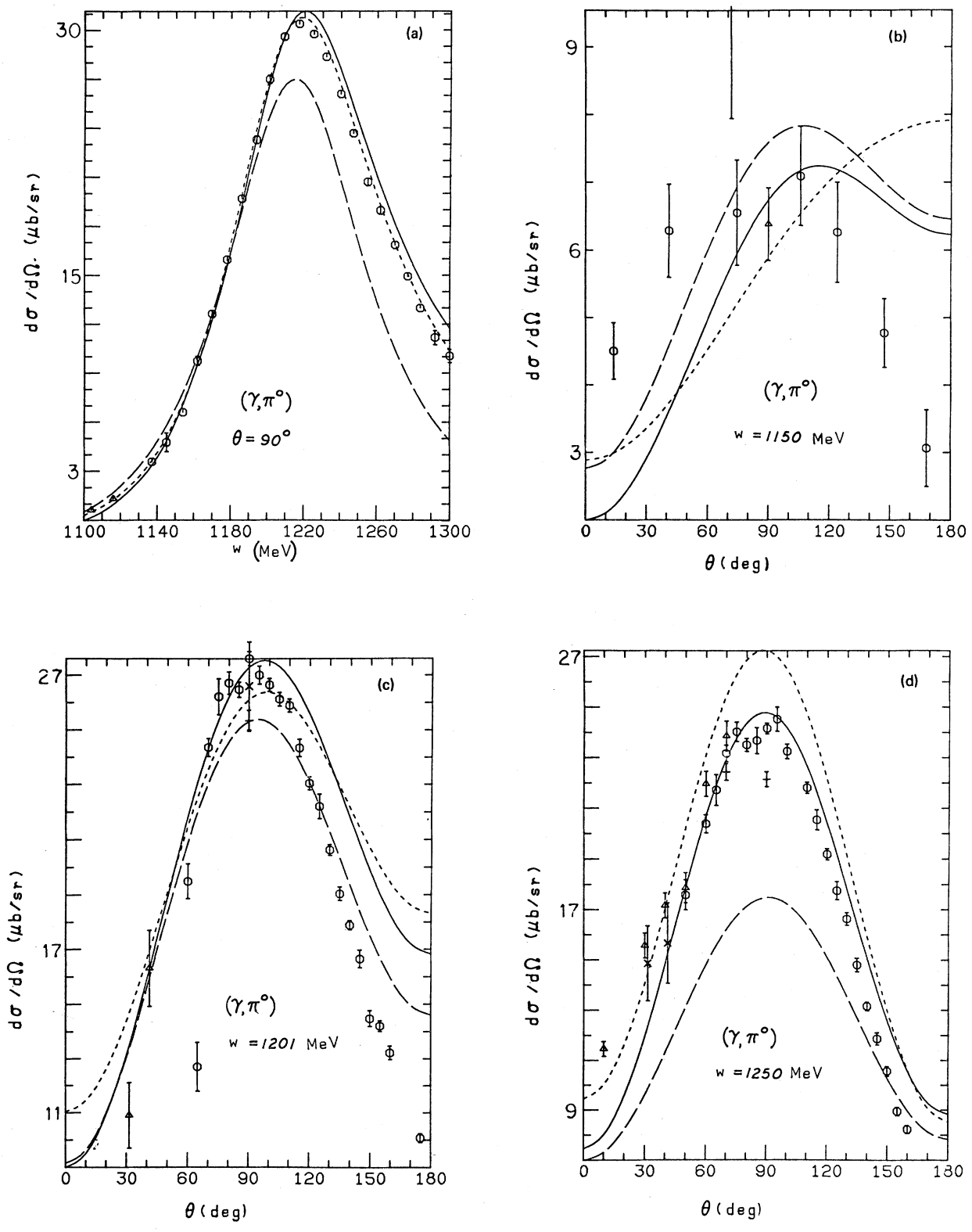

FIG. 5. Differential cross sections for π^0 for (a) $\theta=90$ deg and (b)—(e) for different c.m. energies. Data are from Refs. 25—32.

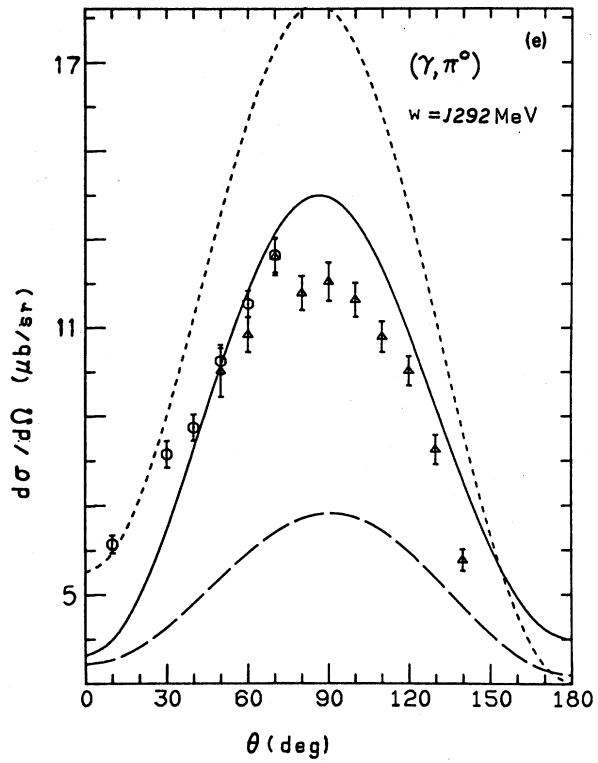

FIG. 5. (*Continued.*)

amplitude follows the data better than BL.

The data in Fig. 10 are from final baryon polarization experiments; the polarization is defined as

$$P=\frac{\frac{1}{2}\sum_{\lambda}\frac{1}{2}[\mathrm{Tr}(F^{+}\vec{\sigma}\cdot\hat{n}F)]}{\frac{1}{2}\sum_{\lambda}\frac{1}{2}[\mathrm{Tr}(F^{+}F)]}\ . \tag{8}$$

$\hat{n}$ is the unit vector in the direction of $\vec{k}\times\vec{q}$, λ labels the polarization state of the photon, $\vec{\sigma}$ is the Pauli spin matrix, and F is the photopion production operator. For this experiment, it is hard to conclude which amplitude reproduces the data. Seen in Fig. 10(b), the new amplitude does follow the data as P changes from positive to negative values.

Except for a small range of energies in Figs. 10(b) and 8(a), negative values of the asymmetry parameters are not obtained from the BL amplitude. The results calculated from the two operators agree in the low c.m. energy regions, with the modified operator giving better results at higher energies. But this trend is not seen in Fig. 8(a); here the BL operator provides the better agreement.

IV. DISCUSSION

Since the calculations with the new and BL photopion production amplitudes yield different results for the $p(\gamma,\pi^0)p$ reaction, the focus of this part of the discussion will be on this neutral reaction. For this reaction, the Δ_{33} in the $I=\frac{3}{2}$ channel is the major contributor to the neutral photopion production amplitude through the M_{1+} multipole. From the Δ_{33} diagram, Fig. 1(b), a M_{1+} multipole is derived by BL:

$$M_{1+}^{\mathrm{BL}}=-\frac{m}{4\pi w}\frac{1}{3}\frac{M_\Delta}{m}\frac{G_1G_3qk}{w^2-M_\Delta{}^2+iM_\Delta\Gamma}\ , \tag{9}$$

where

$$G_1G_3=\left[\frac{(M_\Delta+m)[1+(Rq_\Delta)^2]^{1/2}}{m_\pi{}^2[1+(Rq)^2]^{1/2}}\right]g_1g_3\ , \tag{10}$$

m_π is the pion's mass, k is the magnitude of the photon momentum, q is that of the pion, and q_Δ is the magnitude of the pion momentum at resonant energy. The M_{1+} calculated by Olsson and used in the new photopion production amplitude is given in Eq. (4a). To compare the M_{1+} multipole, Eqs. (4a) and (9) can be put into similar forms:

$$M_{1+}^{\mathrm{BL}}=\frac{N_M^{\mathrm{BL}}}{q}C_{ff}^{\mathrm{BL}}e^{i\delta}\sin(\delta)\ , \tag{9'}$$

$$M_{1+}^{\mathrm{new}}=\left[\frac{N_M}{q}C_{ff}^{\mathrm{new}}\right]e^{i\delta_{33}}\sin(\delta_{33})\ , \tag{4a'}$$

where

$$N_M^{\mathrm{BL}}=\frac{C_0g_1g_3\sqrt{4\pi\alpha}\,(M_\Delta+m)q_\Delta{}^3}{12\pi m_\pi{}^2m_\Delta\Gamma_0}\ , \tag{11}$$

$$C_{ff}^{\mathrm{BL}}=\frac{1}{C_0}\frac{k}{q}\frac{[1+(Rq)^2]^{1/2}}{[1+(Rq_\Delta)^2]^{1/2}}\ , \tag{12}$$

$$\sin(\delta)=\frac{M_\Delta\Gamma}{[(M_\Delta{}^2-w^2)+M_\Delta{}^2\Gamma^2]^{1/2}}\ , \tag{13}$$

$$C_{ff}^{\mathrm{new}}=\cos(\delta_p{}^M-\delta_e)+\cot(\delta_{33})\sin(\delta_p{}^M-\delta_e)\ . \tag{14}$$

$C_0=C_{ff}^{\mathrm{BL}}$ when $w=M_\Delta$; this normalizes C_{ff}^{BL} to 1 when $w=M_\Delta$. In BL, Γ has an energy dependent form to reproduce the δ_{33} experimental pion nucleon phase shifts. The values calculated from Eqs. (4a) and (9) are given in Figs. 3(c) and (d). A comparison of C_{ff}^{new} and C_{ff}^{BL} is given in Fig. 11, where the solid line shows C_{ff}^{new} and the dashed line shows

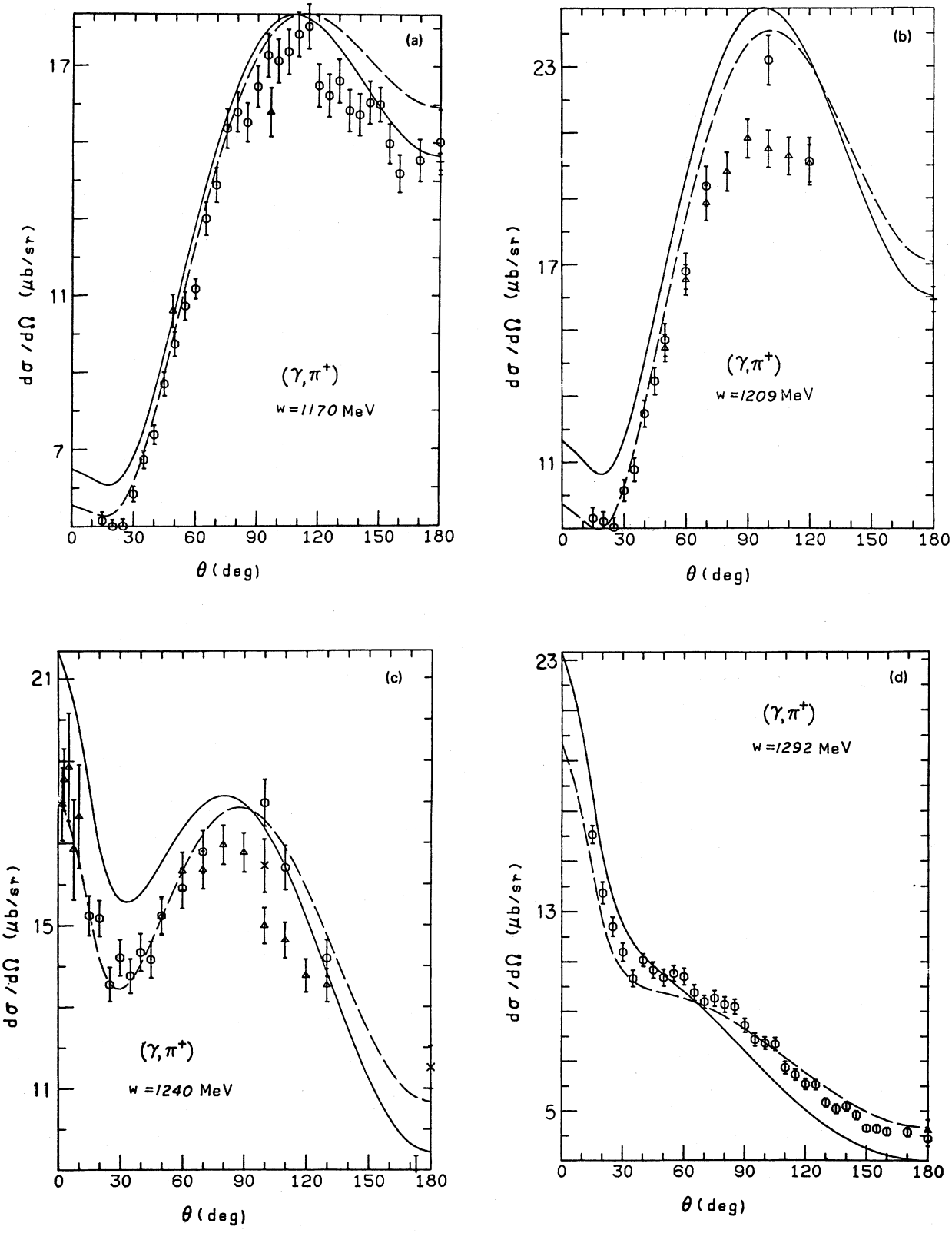

FIG. 6. Differential cross sections for π^+ at different c.m. energies. Data are from Refs. 33–36.

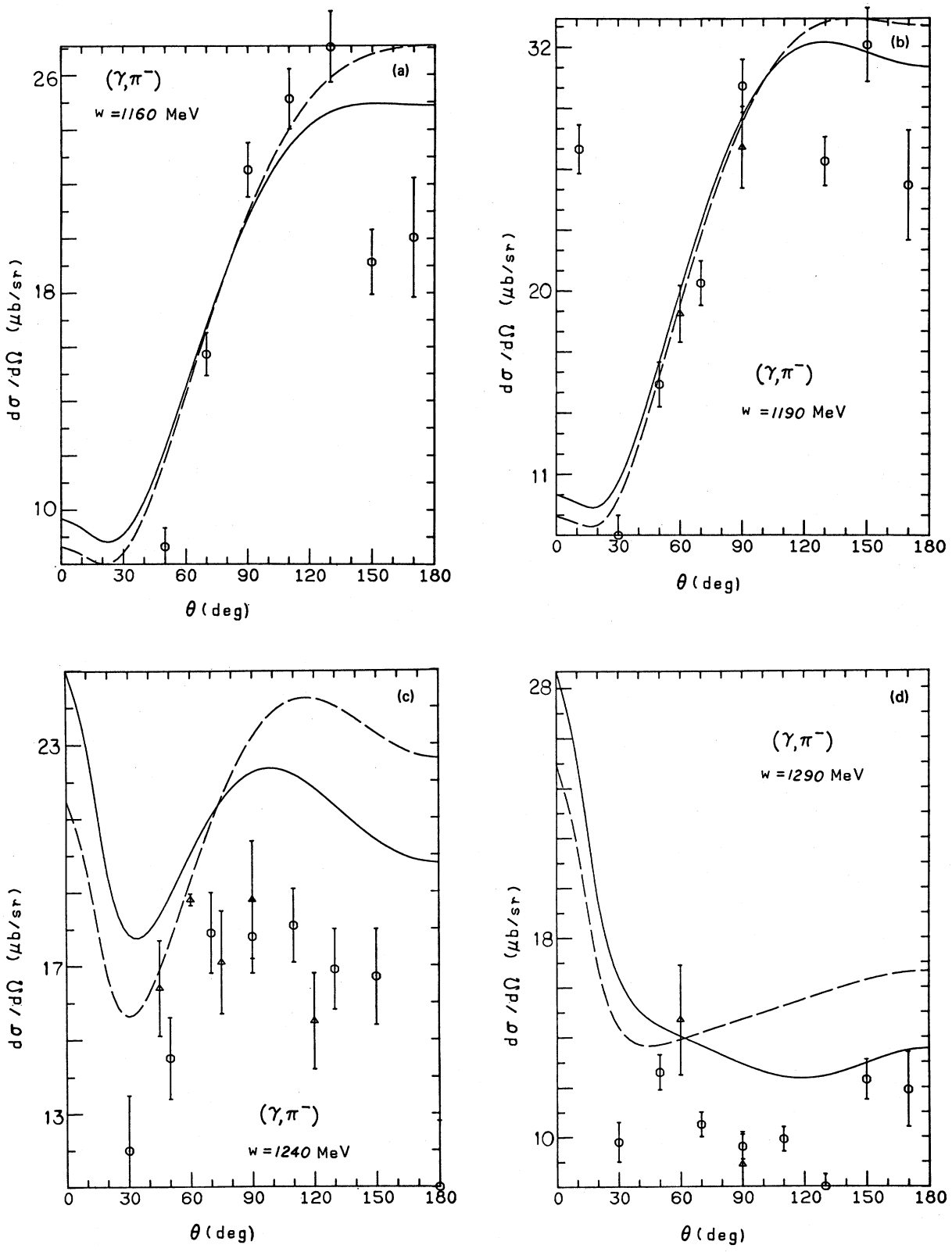

FIG. 7. Differential cross sections for π^- at different c.m. energies. Data are from Refs. 19 and 37.

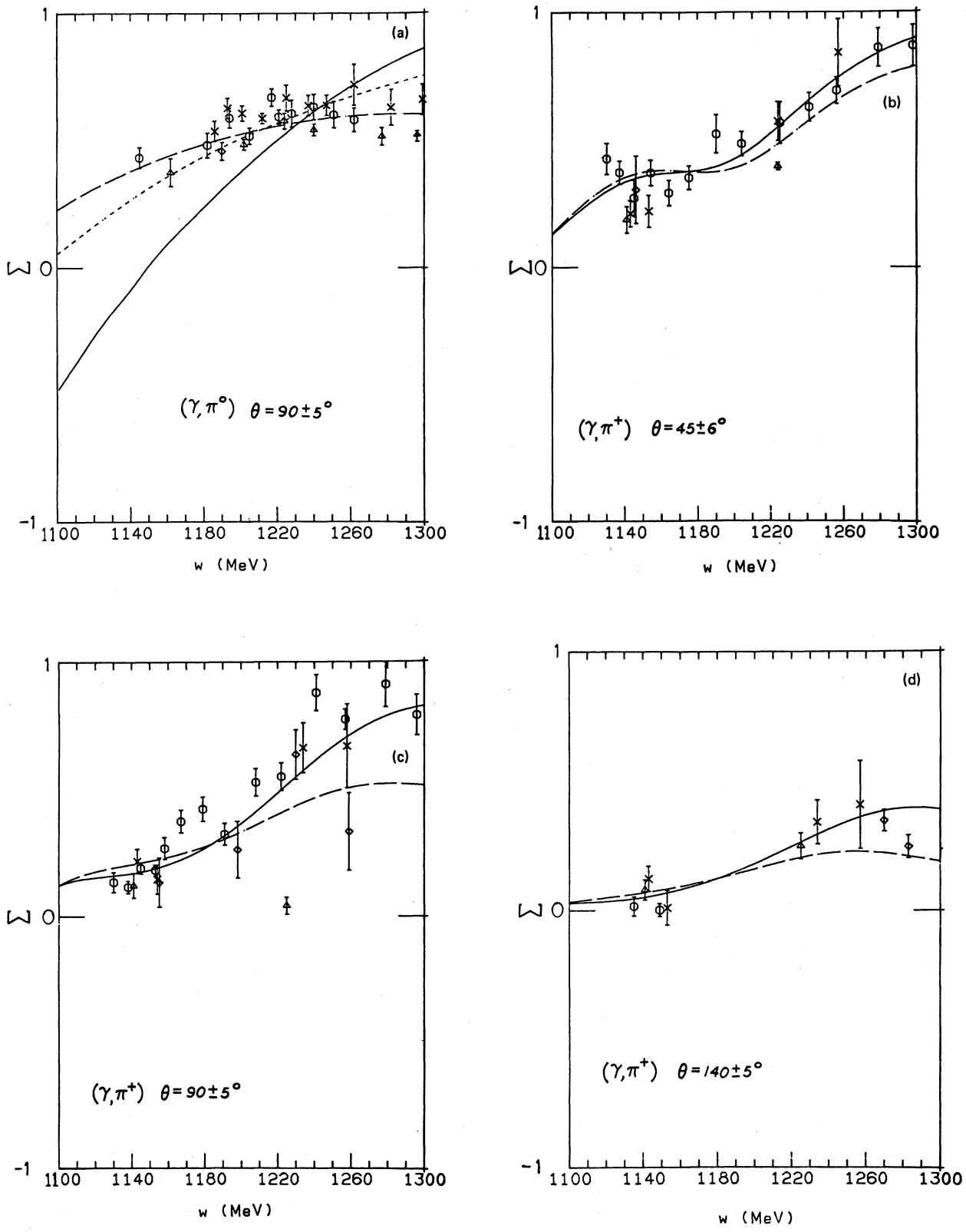

FIG. 8. Photon asymmetry (Σ) for (a) π^0 at $\theta=90\pm5$ deg, π^+ at (b) $\theta=45\pm6$ deg, (c) $\theta=90\pm5$ deg, (d) $\theta=140\pm5$ deg, and (e) π^- at $\theta=90$ deg. Data are from Refs. 38–48.

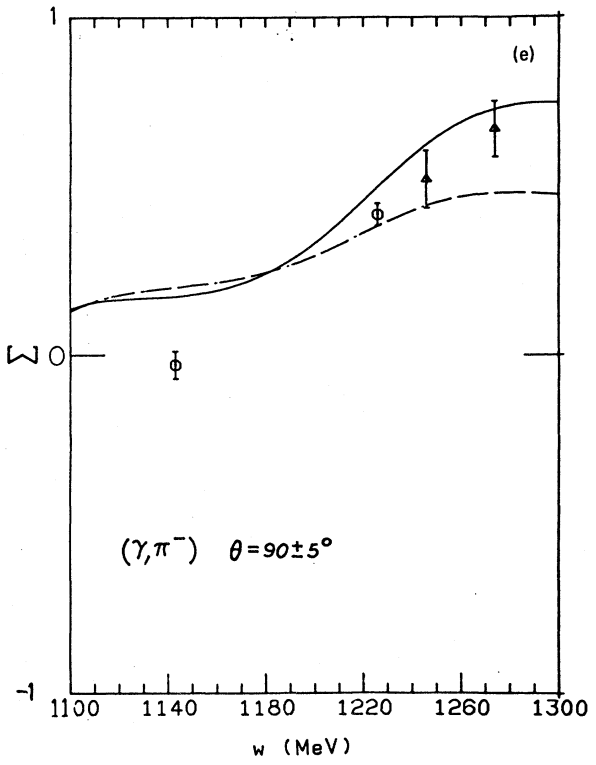

FIG. 8. (*Continued.*)

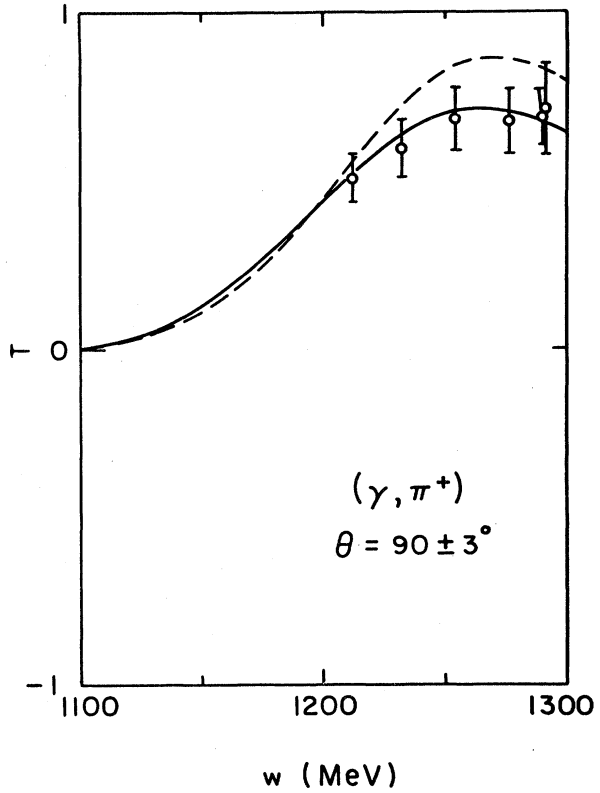

FIG. 9. Target asymmetry (T) for π^+ at $\theta=90\pm3$ deg. Data are from Ref. 49.

C_{ff}^{BL}. If one considers the δ_{33} phase shifts to be entirely attributed to the Δ_{33}, the effects of the background can be included by a modification of C_{ff}^{BL}. What Olsson has shown is that the interference between the Δ_{33} and the background provides an enhancement of this form factor in the 1100—1250 MeV c.m. energy region and a suppression at higher energies.

Because of the large error bars for the polarization data, the new and BL amplitudes both provide an adequate description of these experiments for c.m. energies below the resonance, with the new amplitude providing a better fit at energies above the resonance. However, one exception is seen in Fig. 8(a). In this case, the ω contribution to the photopion production amplitude drives the new amplitude's prediction of the phonon polarization asymmetry parameter, Σ, to negative values. The contribution of the ω meson to photopion production can be ascertained using data from the Σ experiments in the 1100 MeV $< w <$ 1150 MeV energy region. For example, one sees in Fig. 12 different plots for varying ω vertex strengths, $g_{\omega 1}g_{\omega 3}$, for the asymmetry parameter Σ. Using Olsson's model to establish the g_1g_3 vertex strength and the location of the zero for Σ in $p(\gamma,\pi^0)p$, the strength of the product $g_{\omega 1}g_{\omega 3}$ is determined.

Although the new photopion production amplitude provides a better fit to the three types of pion production from a single nucleon considered here, it is not straightforward to put this amplitude into a nuclear framework. The original BL operator has the advantage that the amplitude can be calculated easily in any reference frame, and in each frame the production takes on a differential operator description, but there may be some ambiguities in transforming the new amplitude from the c.m. frame to the laboratory where the initial nucleon is at rest. The extension to electropion production from a single nucleon has been looked at using the original BL operator.[15] Reasonable agreement has been obtained for this case, but preliminary work by this author using the new amplitude extended to electropion production yields results that are too large for the reaction $N(e,e'\pi^0)N$. Further comments on the extension of the new amplitude to electroproduction will be the subject of a future paper.

I would like to thank Dr. Frank Tabakin, Dr. Art Johnson, and Dr. Gregory Toker for helpful discussions.

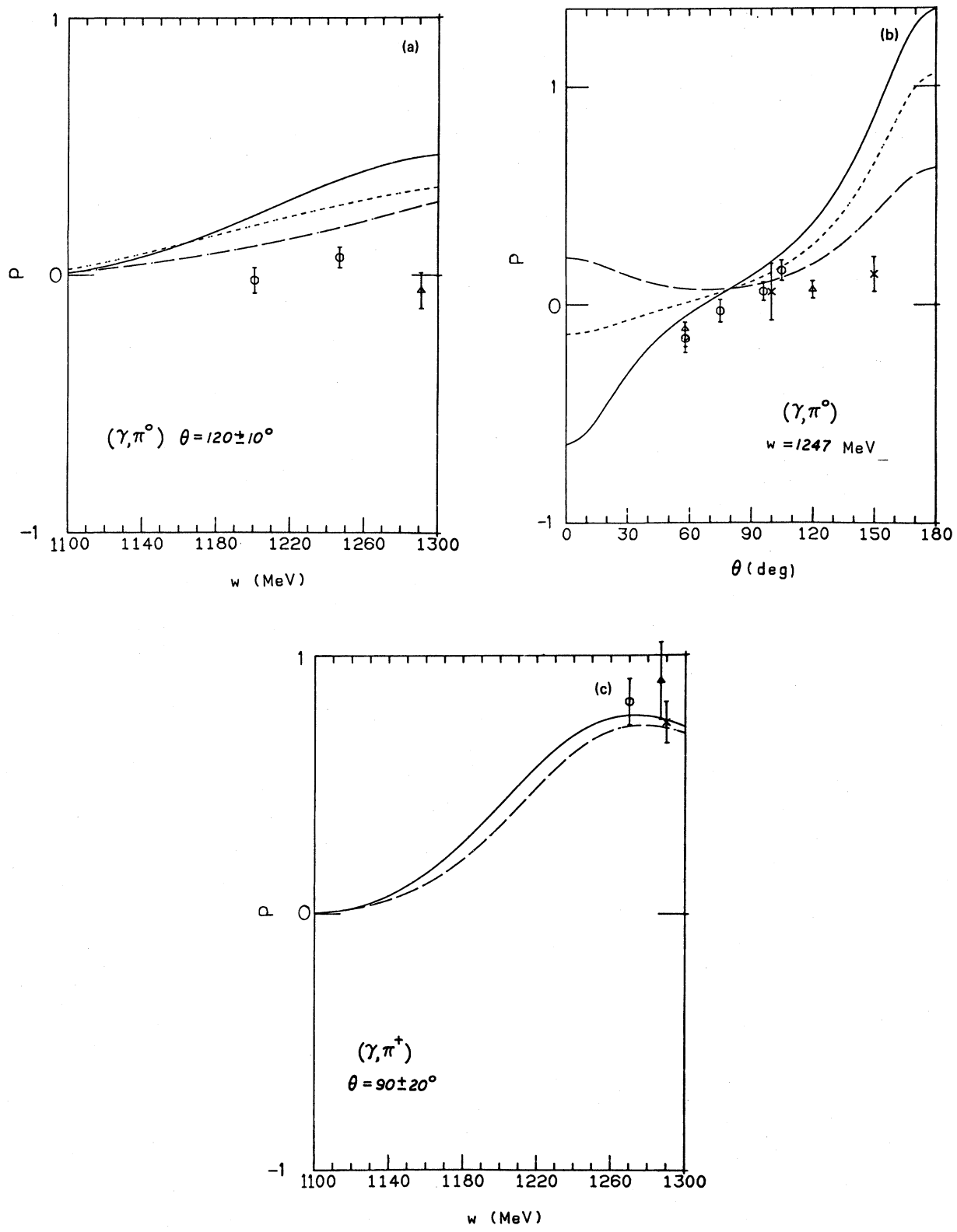

FIG. 10. Final baryon asymmetry (P) for π^0 at (a) $\theta=120\pm10$ deg, (b) $w=1247$ MeV, and π^+ at $\theta=90\pm20$ deg. Data are from Refs. 50–54.

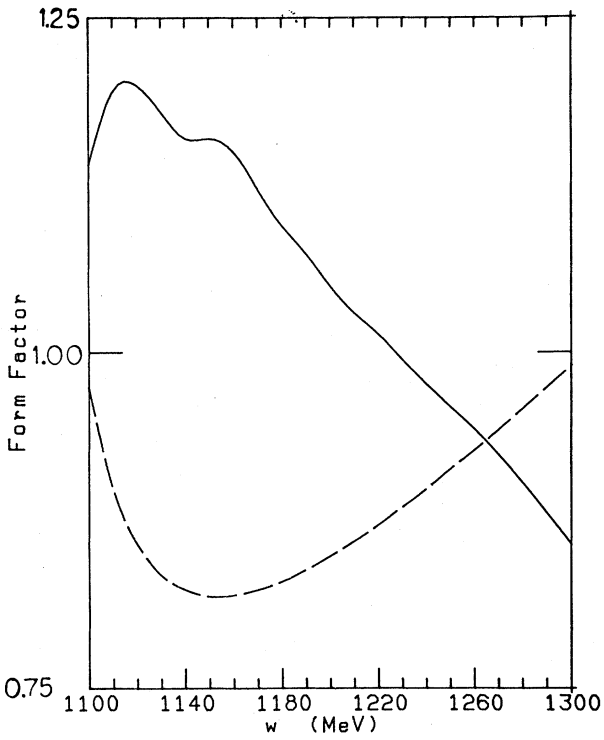

FIG. 11. Comparison of the form factors given in Eq. (12) and (13).

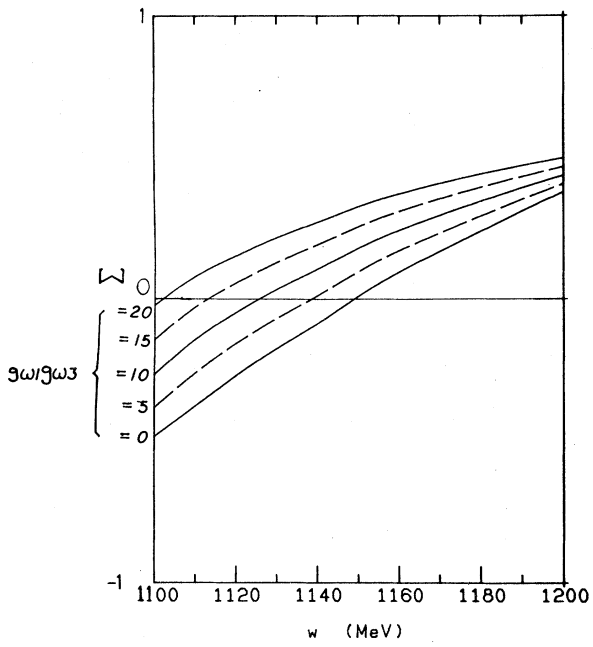

FIG. 12. Plots of Σ for different values of the ω vertex product for the reaction $p(\gamma,\pi^0)p$ at 90 deg.

APPENDIX

In this appendix, the projection of the M_{1+}^{Born} and E_{1+}^{Born} multipoles from the Born contribution to the photopion production amplitude is presented. The explicit forms of the multipoles have been calculated[8] in the c.m. frame of the photon and the initial nucleon in terms of the strengths $F_1 \cdots F_4$, from Eq. (1). The relevant projections are the following:

$$M_{1+}^{\text{Born}}=\tfrac{1}{4}\int_{-1}^{1}dx\left[F_1^{\text{Born}}P_1(x)-F_2^{\text{Born}}P_2(x)-\frac{F_3^{\text{Born}}P_1'(x)(1-x^2)}{2}\right], \tag{A1}$$

$$E_{1+}^{\text{Born}}=\tfrac{1}{4}\int_{-1}^{1}dx\left[F_1^{\text{Born}}P_1(x)-F_2^{\text{Born}}P_2(x)+\frac{F_3^{\text{Born}}P_1'(x)(1-x^2)}{2}+\frac{F_4^{\text{Born}}}{3}\right], \tag{A2}$$

$F_1^{\text{Born}} \cdots F_4^{\text{Born}}$ are the contributions of the Born diagrams [Fig. 1(a)], $P_l(x)$ are the Legendre polynomials, $x=\cos(\theta)$, and the prime denotes differentiation with respect to x. Performing the integration, one finds

$$M_{1+}^{\text{Born}}=\tfrac{1}{16}[\mu_2[f(C,D)-2_g(C,D)]-2e_\pi g(C',D')], \tag{A3}$$

$$E_{1+}^{\text{Born}}=M_{1+}^{\text{Born}}+\tfrac{1}{4}[e_\pi[g(C',D')-\frac{q}{k}h(C',D')]-e_2\frac{q}{k}h(C,D)+\mu_2 g(C,D)]\,. \tag{A4}$$

μ_2 is the total magnetic moment of the final state nucleon, e_2 is 1 or 0 depending on whether the final state nucleon is a proton or neutron, and e_π is 1, -1, or 0 depending on whether the produced pion is π^+, π^-, or π^0, respectively. The functions f, g, and h are the following:

$$f(x,y)=2\frac{x}{y}-(1+x^2)\ln\frac{x+y}{x-y}, \tag{A5}$$

$$g(x,y)=2\frac{x}{y}+(1-x^2)\ln\frac{x+y}{x-y}, \tag{A6}$$

$$h(x,y)=\frac{4}{3}-2\frac{x^2}{y^2}-\frac{x}{y}\left[1-\frac{x^2}{y^2}\right]\ln\frac{x+y}{x-y}\ . \tag{A7}$$

C, D, C', and D' are functions of the energies of the photon and pion, k_0 and q_0, the magnitude of the momenta of the photon and pion, k and q, and the nucleon mass m:

$$C=-2m\left[k_0+\frac{k^2}{2m}\right], \tag{A8}$$

$$D=-D'=-2qk\ , \tag{A9}$$

$$C'=-2k_0q_0\ . \tag{A10}$$

Inverting the isospin decomposition of the F_i, given by Eqs. 2(a)—(d), to obtain the form of the multipole in the $I=\frac{3}{2}$ channel, one finds

$$f_{LJ}(I=\tfrac{3}{2})=f_{LJ}(\gamma p\to p\pi^0)-\frac{1}{\sqrt{2}}f_{LJ}(\gamma p\to n\pi^+)\ . \tag{A11}$$

The final result is then:

$$M_{1+}^{\text{Born}}(I=\tfrac{3}{2})=\tfrac{1}{16}\left[\left[\mu_p-\frac{\mu_n}{\sqrt{2}}\right][f(C,D)-2g(C,D)]+\sqrt{2}g(C',D')\right], \tag{A12}$$

$$E_{1+}^{\text{Born}}(I=\tfrac{3}{2})=\tfrac{1}{16}\left[\left[\mu_p-\frac{\mu_n}{\sqrt{2}}\right][f(C,D)+2g(C,D)]-4\frac{q}{k}h(C,D)-\sqrt{2}[g(C',D')-2\frac{q}{k}h(C',D')]\right]. \tag{A13}$$

[1]K. I. Blomqvist and J. M. Laget, Nucl. Phys. B280, 405 (1977).

[2]M. K. Singham and F. Tabakin, Ann. Phys. (N.Y.) 135, 71 (1981).

[3]M. K. Singham, Ph.D. dissertation, University of Pittsburgh, 1981.

[4]G. W. Reynaud and F. Tabakin, Phys. Rev. C 23, 2652 (1981).

[5]D. Rawley *et al.*, Phys. Rev. C 25, 2652 (1982).

[6]For a list of parameters, see Table I.

[7]M. G. Olsson, Phys. Rev. D 13, 2505 (1976).

[8]S. Fubini, Y. Nambu, and V. Wataghin, Phys. Rev. 111, 329 (1958).

[9]Philippe Dennery, Phys. Rev. 124, 2000 (1961).

[10]G. F. Chew, M. L. Goldberger, F. E. Low, and Y. Nambu, Phys. Rev. 106, 1345 (1957).

[11]K. M. Watson, Phys. Rev. 95, 228 (1954).

[12]M. G. Olsson and E. T. Osypowski, Nucl. Phys. B87, 339 (1975).

[13]M. G. Olsson, Leaf Turner, and E. T. Osypowski, Phys. Rev. D 7, 3444 (1973).

[14]M. G. Olsson and E. T. Osypowski, Nucl. Phys. B101, 136 (1975).

[15]S. Mehrotra and L. E. Wright, Nucl. Phys. A362, 481 (1981).

[16]J. R. Carter, D. V. Bugg, and A. A. Carter, Nucl. Phys. B58, 378 (1973).

[17]F. A. Berends and A. Donnachie, Nucl. Phys. B84, 342 (1974).

[18]W. Pfeil and D. Schwela, Nucl. Phys. B45, 379 (1972).

[19]P. Benz *et al.*, Nucl. Phys. B65, 158 (1973).

[20]L. H. Guex *et al.*, Phys. Lett. 55B, 101 (1975).

[21]G. van Holtey, G. Knop, H. Stein, J. Stumpfig, and H. Wahlen, Phys. Lett. 40B, 589 (1972).

[22]G. van Holtey, G. Knop, H. Stein, J. Stumpfig, and H. Wahlen, Nucl. Phys. B70, 379 (1974).

[23]T. Fujii *et al.*, Phys. Rev. Lett. 28, 1672 (1972).

[24]T. Fujii *et al.*, Phys. Rev. Lett. 29, 244 (1972).

[25]G. Fischer *et al.*, Nucl. Phys. B16, 93 (1970).

[26]W. Hitzenroth, Nuovo Cimento 60, 467 (1969).

[27]B. B. Govorkov, S. P. Denison, and E. V. Minarik, J. Nucl. Phys. (U.S.S.R.) 6, 370 (1968).

[28]G. Bernardini, O. A. Hanson, A. C. Odian, T. Yamagata, L. B. Auerbach, and I. Filosofo, Nuovo Cimento 18, 1203 (1960).

[29]D. B. Miller and E. H. Bellany, Proc. Phys. Soc., London 81, 343 (1963).

[30]W. S. McDonald, V. Z. Peterson, and D. R. Corson, Phys. Rev. 107, 577 (1957).

[31]R. Morand, E. F. Erickson, J. P. Pahin, and M. G. Crossiaux, Phys. Rev. 180, 1299 (1969).

[32]Z. Higler, L. Simions, and M. Tonutti, University of Bonn, Report P1B1-103, 1970.

[33]G. Fischer, H. Fischer, M. Heuel, G. von Holtey, G. Knop, and J. Stumpfig, Nucl. Phys. B16, 119 (1970).

[34]B. Bouquet *et al.*, Phys. Rev. Lett. 27, 1244 (1971).

[35]C. Betourni *et al.*, Phys. Rev. 172, 1343 (1968).
[36]T. Fujii *et al.*, Phys. Rev. Lett. 26, 1672 (1972).
[37]L. H. Guex *et al.*, Phys. Lett. 55B, 101 (1975).
[38]P. Blum *et al.*, in *Fourth International Symposium on Electron and Photon Interactions at High Energy, Liverpool, 1969,* edited by D. W. Braben and R. E. Rand (Daresbury Nuclear Physics Laboratory, Daresbury, England, 1970).
[39]Yu. Antufyev, *et al.*, MIT-SLAC Report No. SLAC-PUB-796, 1970 (unpublished), presented at the Fifteenth International Conference on High Energy Physics, Kiev, U.S.S.R., 1970.
[40]G. Bolongna, F. L. Fabbri, P. Spillantini, and V. Valenti, Frascati, Report LNF-70/39, 1970.
[41]D. J. Drickey and R. F. Mozley, Phys. Rev. 136, B543 (1964).
[42]R. W. Zdarko and E. B. Dalley, Nuovo Cimento 10A, 10 (1972).
[43]N. C. Grilli, P. Spillantini, F. Soso, M. Nigro, E. Schiavuta, and V. Vanlenti, Nuovo Cimento 54, 877 (1968).
[44]F. F. Liu, D. J. Drickey, and R. F. Mozely, Phys. Rev. 136, B1183 (1964).
[45]R. C. Smith and R. F. Mozley, Phys. Rev. 130, 2429 (1963).
[46]V. M. Kuznetsov, J. Nucl. Phys. (U.S.S.R.) 13, 603 (1971).
[47]R. E. Taylor and R. F. Mozley, Phys. Rev. 117, 835 (1960).
[48]K. Kondo, T. Nishikawa, T. Suzuki, K. Takikawa, H. Yoshida, Y. Kimura and M. Kobayashi, J. Phys. Soc. Jpn. 29, 13 (1970).
[49]S. Arai *et al.*, Nucl. Phys. B48, 397 (1972).
[50]K. H. Althoff, D. Finken, N. Minatti, H. Piel, D. Trines, and M. Unger, Phys. Lett. B26, 677 (1968).
[51]R. L. Walker, see Ref. 38.
[52]S. Hayakawa *et al.*, J. Phys. Soc. Jpn. 25, 307 (1968).
[53]K. H. Althoff, K. Kramp, H. Matthay, and H. Piel, *Proceedings of the International Symposium on Electron and Photon Interactions at High Energies, Hamburg, 1965* (Springer, Berlin, 1965), p. 286.
[54]W. Wallraff, Ph.D. dissertation, University of Bonn, 1972.